

# Synthesis, characterization and lithium electrochemical insertion into antimony-based graphite composites

Anne Dailly<sup>a</sup>, Jaafar Ghanbaja<sup>a</sup>, Patrick Willmann<sup>b</sup>, Denis Billaud<sup>a,\*</sup>

<sup>a</sup> LCSM, UMR CNRS 7555, Université Henri Poincaré Nancy I, BP 239, Vandoeuvre les Nancy Cédex 54506, France

<sup>b</sup> Centre National d'Etudes Spatiales, Avenue E. Belin, 31055 Toulouse Cédex, France

Available online 18 May 2004

## Abstract

There is a renewal of interest in the use of metals that are capable of alloying with lithium as negative-electrode materials for lithium-ion batteries. These metals can supply larger capacities than graphite but their main disadvantage consists in their very limited cycle life.

Indeed, they present considerable volume variations during alloying, which lead to a mechanical degradation of the electrode. The concept of an active phase stabilizing matrix was introduced. We propose in this study to associate a metal able to alloy lithium to graphite by using new preparation methods involving graphite intercalation compounds (GICs) as precursors.

In one case, antimony pentachloride  $\text{SbCl}_5$  was reduced by the stage I  $\text{KC}_8$  GIC. In another case,  $\text{C}_{12}\text{SbCl}_5$  and  $\text{C}_{24}\text{SbCl}_5$  GICs were reduced either by gaseous caesium or by activated sodium hydride NaH. Actually, these methods led to the attention of antimony-based graphite composites in which antimony particles are deposited on the surface and edges of graphite layers or embedded in an organic matrix. Both morphological and structural characteristics of such composites were studied by transmission electron microscopy. Examination of their electrochemical properties as regards lithium insertion showed that they present interesting performances because the reversible capacity is increased by comparison with that of pure graphite and the stability of the metal is preserved throughout the cycling. The combination of graphite and antimony prevents the metal against cracking and pulverization that occur generally during alloying/dealloying cycles. Antimony-graphite composites prepared via  $\text{SbCl}_5$  reduction by  $\text{KC}_8$ , via  $\text{C}_{12}\text{SbCl}_5$  reduction by gaseous caesium or via  $\text{C}_{24}\text{SbCl}_5$  reduction by activated NaH display improved reversible capacities of 420, 490 and 440  $\text{mAh g}^{-1}$ , respectively.

© 2004 Elsevier B.V. All rights reserved.

**Keywords:** Lithium intercalation; Lithium–antimony alloys; Rechargeable lithium-ion battery

## 1. Introduction

Increasing the specific energy and the cell cycle life of lithium-ion batteries is a continuous challenge. Within negative electrode materials used, graphite is a reference material which provides a theoretical specific charge of  $372 \text{ mAh g}^{-1}$  corresponding to the formation of the stage I  $\text{LiC}_6$  graphite intercalation compound. Moreover, the low volume expansion ( $\approx 10\%$ ) of graphite during lithium intercalation allows the electrode to maintain its dimensional stability and to provide good cycling performances. The irreversible specific charge in the first cycle of graphite electrodes corresponds mainly to the formation of the solid electrolyte interphase and is now limited to about 7% of the theoretical capacity.

This capacity can be improved by substituting graphite by low temperature hard (non-graphitizable) and soft (graphiti-

zable) carbons. However, in many cases, such carbons display an important irreversible capacity in the first cycle and a strong hysteresis between the charge and discharge cycles resulting in a drastic loss of the cell specific energy. Moreover, the reversible specific charge is often random since it depends on many parameters like the nature and the content of heteroelements, the type of porosity (accessibility and pore size) and the extent of the structural disorder [1].

Recently, investigations of metal oxides and/or metal-based negatives electrodes have received considerable attention due to the high expected specific charges [2–5]. However, most of these systems suffer from a systematic loss of capacity upon cycling due, in part, to the important volume variations accompanying lithium alloying and dealloying. These large volume changes associated with the ionic character of the lithium alloys which are therefore brittle, induce a rapid decay in mechanical properties and the irreversible degradation by pulverization of the electrode. The use of thin films of metal or of nanosized metal particles embedded in an active or inactive matrix allows to over-

\* Corresponding author. Tel.: +33-3-83-68-46-22;

fax: +33-3-83-68-46-23.

E-mail address: [denis.billaud@lcsm.uhp-nancy.fr](mailto:denis.billaud@lcsm.uhp-nancy.fr) (D. Billaud).

come partly the consequence of these mechanical stresses [6–8].

In this communication, we present methods showing how graphite intercalation compounds can be used as precursors for the elaboration of new graphite–metal compounds in which both graphite and metal are able to insert lithium. Among these methods, one consists in the reduction of metal halide graphite intercalation compounds by reducing species like alkali metals or alkaline hydrides activated in organic media [9–11]; in another method, metal halides are reduced by an alkali metal graphite intercalation compound like  $\text{KC}_8$  for instance [12].

The graphite–metal composites obtained via graphite intercalation compounds have been characterized by transmission electron microscopy. Their electrochemical performances as regards to lithium insertion have been estimated both in galvanostatic and voltammetric modes.

## 2. Results and discussion

Fig. 1a shows the bright field micrograph and the related electron diffraction pattern of a graphite–antimony compos-

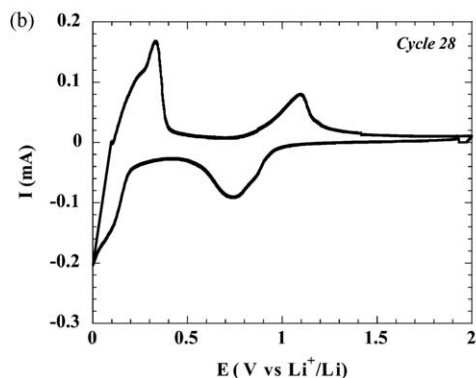
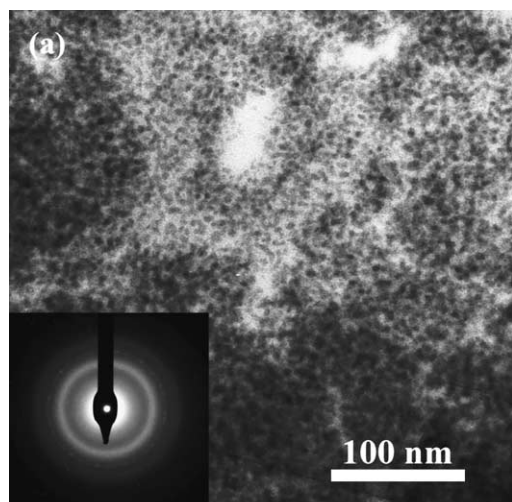


Fig. 1. Graphite–Sb compound obtained after reduction of  $\text{C}_{24}\text{SbCl}_5$  by activated NaH: bright field micrograph and related electron diffraction pattern (a); corresponding cyclic voltammogram in  $\text{LiClO}_4$  (1 M)-EC (b).

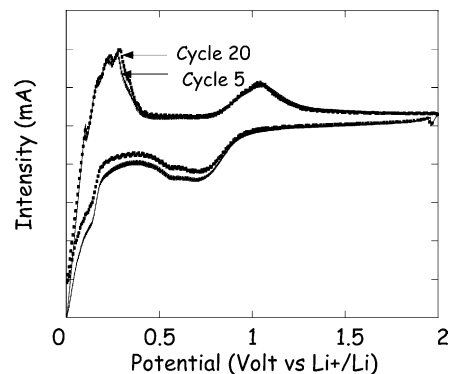
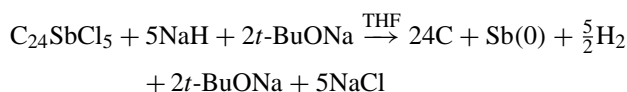


Fig. 2. Selected cyclic voltammogram of the graphite–Sb composite obtained by reduction of  $\text{C}_{12}\text{SbCl}_5$  by caesium ( $\text{LiClO}_4$  (1 M)-EC).

ite material obtained after reduction of a stage II  $\text{C}_{24}\text{SbCl}_5$  graphite intercalation compound by NaH activated in an organic medium. The chemical reaction we employed for the preparation of Sb nanoparticles using *t*-BuONa activated NaH and  $\text{SbCl}_5$  can be formulated as:



This material was washed in ethanol and water in order to remove both unreacted NaH and NaCl formed as a side product. The composite material is formed of antimony nanoparticles dispersed uniformly in an organic matrix. The electron diffraction pattern shows a broad and low intense ring indexed as the 0 1 2 reflection of antimony indicating the amorphous character of this metal. Fig. 1b shows a cyclic voltammogram of this graphite–Sb-based composite. The low potential peaks are related to lithium intercalation into graphite to form  $\text{LiC}_6$  while the peaks around 0.9 versus  $\text{Li}^+/\text{Li}$  correspond to lithium alloying into Sb with formation of the  $\text{Li}_3\text{Sb}$  compound. Note that the reversible specific charge of this graphite–antimony material is close to  $440 \text{ mAh g}^{-1}$ . Starting with a stage I  $\text{C}_{12}\text{SbCl}_5$  material

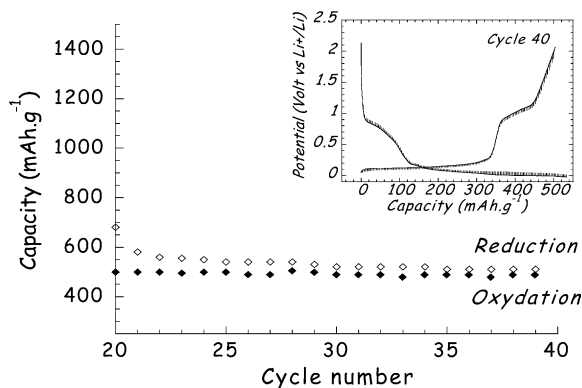


Fig. 3. Variation of irreversible and reversible capacities as a function of the cycle number for the compound of Fig. 2. The inset shows the voltage profile of the 40th cycle.

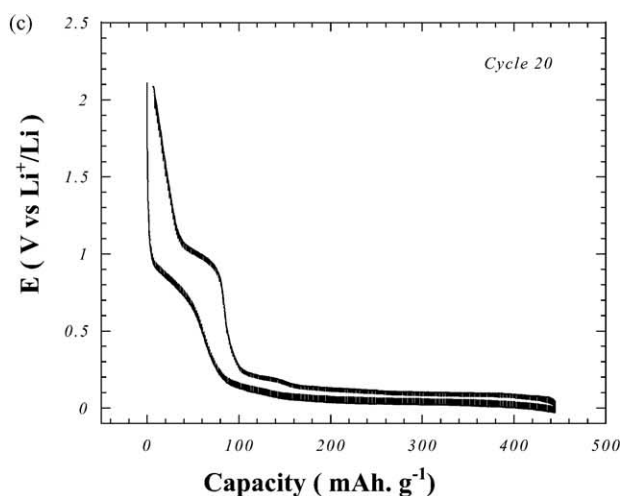
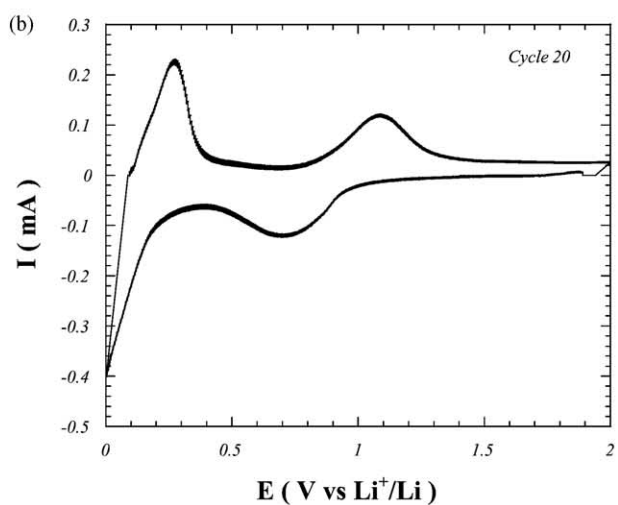
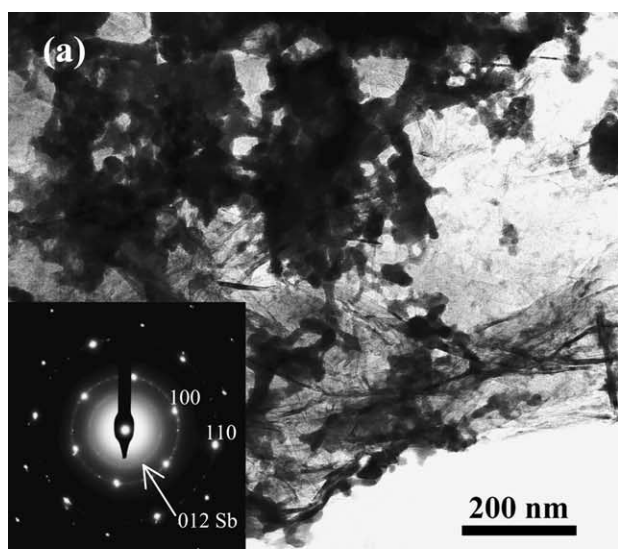
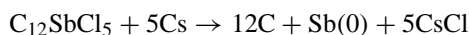


Fig. 4. Graphite–Sb compound obtained after reduction of  $\text{SbCl}_5$  by  $\text{KC}_8$ : bright field micrograph and related electron diffraction pattern (a); the corresponding cyclic voltammogram (b) and voltage vs. capacity plots (c) (current density:  $7 \mu\text{A}/\text{mg}$ ) in  $\text{LiClO}_4$  (1 M)-EC.

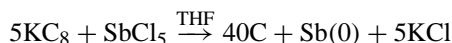
leads to a reversible specific charge of  $492 \text{ mAh g}^{-1}$  according to the increase of Sb content in the composite material.

Similar results were obtained by reducing a  $\text{C}_{12}\text{SbCl}_5$  graphite intercalation compound by caesium in the vapour phase according to the following reaction:



The resulting graphite/Sb composite presented not only an improved storage capacity ( $490 \text{ mAh g}^{-1}$ ) but also an enhanced dimensional stability of lithium–antimony alloys. Fig. 2 presents for instance selected cyclic voltammograms of such a graphite–Sb composite while Fig. 3 shows the variation of both irreversible and reversible capacities versus the cycle number. The inset in Fig. 3 presents the voltage profile of the 40th cycle.

Fig. 4a presents the bright field micrograph and the corresponding electron diffraction pattern of a graphite–antimony material obtained after reduction in THF of  $\text{SbCl}_5$  by  $\text{KC}_8$  according to the following equation:



A washing with a water/ethanol mixture allows to eliminate KCl formed as a side reaction product. Nanosized antimony particles appear as small aggregates deposited on the graphite surface. The electron diffraction pattern shows the broad ring of amorphous antimony (012 reflections) and the characteristic  $hk0$  reflections of graphite. Fig. 4b and c present a cyclic voltammogram and a galvanostatic charge/discharge of such a graphite–Sb composite. In both cases, two series of reversible transformations are present: lithium intercalation into graphite at the lowest potentials and lithium alloying into antimony at the highest potentials. The reversible specific charge of this graphite–antimony composite is close to  $420 \text{ mAh g}^{-1}$ .

### 3. Conclusion

Novel processes using graphite intercalation compounds have been described to synthesize antimony/graphite composites.

Reduction of a  $\text{SbCl}_5$ –graphite intercalation compound by activated NaH leads to a complex material composed of amorphous antimony nanoparticles embedded in an organic matrix and supported on graphite. Reduction of the same GIC by gaseous caesium results in the formation of Sb/graphite composite in which film-like antimony aggregates are present on the graphite surface. Finally,  $\text{SbCl}_5$  reduction by  $\text{KC}_8$  leads to Sb/graphite composites exhibiting also film-like antimony particles deposited on the graphite surface.

Electrochemical lithium insertion has been carried out in these materials. Reversible lithium insertion/deinsertion occurs both in graphite and in antimony. The reversible specific charge is increased by comparison with that of pure graphite

and the metal stability is preserved throughout the cycling. The combination of graphite and antimony obtained with our techniques prevents the metal against cracking that usually occurs during lithium alloying/dealloying. A possible bond between amorphous antimony and graphite could be responsible for such improved performances upon cycling. Such an hypothesis remains to be supported by using suitable characterizations (EELS, Mössbauer spectroscopy) and also by studying other metal/graphite composites obtained by the same synthesis methods.

## References

- [1] J.R. Dahn, T. Zheng, Y. Liu, J.S. Hue, *Science* 270 (1995) 590.
- [2] Y. Idota, T. Kubota, A. Matsfujii, Y. Maekawa, T. Miyasaka, *Science* 276 (1997) 1395.
- [3] J. Yang, M. Winter, J.O. Besenhard, *Solid State Ionics* 90 (1996) 281.
- [4] A. Ulms, Y. Rosenberg, L. Burstein, E. Peled, *J. Electrochem. Soc.* 149 (2002) A635.
- [5] J. Yang, Y. Takeda, N. Imanishi, O. Yamamoto, *J. Electrochem. Soc.* 146 (1999) 4009.
- [6] J. Read, D. Foster, J. Wolfenstine, W. Behl, *J. Power Sources* 96 (2001) 277.
- [7] O. Mao, R.L. Turner, I.A. Courtney, B.D. Fredericksen, M.I. Buckett, L.J. Krause, J.R. Dahn, *Electrochem. Solid State Lett.* 2 (1999) 3.
- [8] J.Y. Lee, R. Zhang, Z. Liu, *J. Power Sources* 90 (2000) 70.
- [9] A. Dailly, R. Schneider, D. Billaud, Y. Fort, P. Willmann, *Electrochim. Acta* 47 (2002) 4207.
- [10] A. Dailly, R. Schneider, D. Billaud, Y. Fort, J. Ghanbaja, *J. Nanoparticle Res.* 5 (3) (2003) 389.
- [11] A. Dailly, J. Ghanbaja, P. Willmann, D. Billaud, *J. Power Sources* 125 (1) (2004) 70.
- [12] A. Dailly, J. Ghanbaja, P. Willmann, D. Billaud, *Electrochim. Acta* 48 (2003) 977.